A SCALING CONSTANT EQUAL TO UNITY IN 1D QUADRATIC MAPS

M. ROMERA, G. PASTOR and F. MONTOYA

Instituto de Física Aplicada, Consejo Superior de Investigaciones Científicas,
Serrano 144, 28006 Madrid, Spain
e-mail: gerardo@iec.csic.es

Abstract—

Presumably, there are an infinity of scaling constants in 1D quadratic maps; therefore, it is meaningless to try to find all of them. However, some of these constants that have contributed to a better knowledge of the 1D quadratic maps have been published. In this work we illustrate some of the central features of the most important scaling constants and we introduce another one which has the notable property that its value, numerically obtained, presumably is unity.

1. INTRODUCTION

In 1978, M. J. Feigenbaum published his famous article [1] where for the first time he defined and computed the scaling constant, δ_F, in the period-doubling cascade of 1D maps with a unique maximum. In the appendix B of [1] the method used to obtain the constant is very concisely described. However, when we seek to obtain the constant, serious difficulties appear, and the works of Briggs [2,3] can be very useful to overcome these difficulties. According to Peitgen *et al.* [4], at first glance it may seem very difficult to compute the parameter sequence from which δ_F can be estimated and, however, Feigenbaum performed his first experiments merely using a pocket calculator, and it is not black magic at all. Being aware of this difficulty, Peitgen *et al.* explained in detail the procedure of Feigenbaum for the computation of δ_F [4].

Besides the scaling constant of Feigenbaum, many more scaling constants –maybe an infinite number of them– can be found. Therefore, finding another new scaling constant seems to be of no interest. However, some scaling constants which are important for a better knowledge of 1D quadratic maps have been published. In this work we will introduce a new scaling constant and we conjecture that its value is unity.

As is well known, all the 1D quadratic maps are equivalent because they are topologically conjugate [4-6] . This means that any 1D quadratic map can be used to study the others; we chose the real Mandelbrot map $x_{n+1} = x_n^2 + c$. Recently, to study this map [7-10], we have used the real axis neighborhood (the antenna) of the Mandelbrot set that offers graphic advantages [11]. However, we must take into account that only the intersection of the Mandelbrot set and the real axis have a sense in the study of the real Mandelbrot map. In this work we shall apply again this technique in order to illustrate some of the central features of the scaling constants.

2. PREVIOUS CONSIDERATIONS

2.1. About the computer precision

In a 1D quadratic map it is possible to find sequences of superstable points, of Misiurewicz points or of other points. As is well known these sequences are, in the limit, decreasing geometric progressions with a scaling constant equal to the inverse of the ratio of the progression.

Let c_0, c_1, …, c_{n-1}, c_n, c_{n+1}, … be the parameter values of a sequence of points (see Fig. 1). As is well known, the scaling constant of this sequence can be defined as $\delta = \lim_{n\to\infty} |c_n - c_{n-1}| / |c_{n+1} - c_n|$. To measure this scaling constant we calculate the values $\delta_1 = |c_1 - c_0| / |c_2 - c_1|, \ldots,\ \delta_n = |c_n - c_{n-1}| / |c_{n+1} - c_n|, \ldots$ until we reach the desired precision [1].

In this calculus procedure the precision of the computer is crucial, which is estimated by means of the *machine accuracy* [12] or the *machine unit* [4]. The computer used in this work has a machine accuracy of 5.2×10^{-18}, and a machine unit of $2^{-57} = 6.9 \times 10^{-18}$, i.e., 17 significant decimal digits. However, these 17 significant decimal digits are not 17 "good" decimal digits (the arithmetic among numbers in floating-point representation is not exact [12]), as can easily be seen by carrying out additions and multiplications for tests (addition and multiplication are the only two needed operations to iterate the map $x_{n+1} = x_n^2 + c$). So, in Table 1 the calculus precision for two multiplications is tested. In the computed values, the 17th and 16th decimal

digits are incorrect in both operations; whereas, the 15th decimal digit is exact in the first and quasi exact in the second one. In accordance with that, we shall give the results of this work with 15 significant decimal digits.

At the beginning, when *n* is small, the values calculated of δ_n are more and more precise when *n* increases, but afterwards, as can be observed, the precision decreases. It makes no sense to continue the calculus of δ_n for larger indices *n*, because the change in consecutive values of *c*, i.e. $|c_n - c_{n-1}|$ will have less than half as many significant digits, which signal large errors in the computation of δ_n due to cancellation of digits [4]. We shall give the values of the constants with 6 decimal digits at most.

2.2. About the symbolic sequences

We write the symbolic sequence of the period-3 superstable orbit of the real Mandelbrot map, located at $c = -1.754877666246692\ldots$, as CLR. The first letter (C) corresponds to $x_0 = 0$, the second one (L) corresponds to $x_1 < 0$, and the third one (R) corresponds to $x_2 > 0$. Then, the symbolic sequence of the period-8 superstable orbit, located at $c = -1.711079470013152\ldots$, is $\mathrm{CLRLLRLL} = \mathrm{C}\overline{\mathrm{LRL}}^{2}\mathrm{L}$ (we only use brackets in symbolic sequences of Misiurewicz points). As another example, the symbolic sequence of the period-16 superstable orbit of the period-doubling cascade, located at $c = -1.396945359704560\ldots$, is $\mathrm{CLRL}^3\mathrm{RLRLRL}^3\mathrm{RL}$. As is well know, the symbolic sequence of a periodic orbit, for a given parameter value, can easily be obtained by direct iteration.

The symbolic sequence of the orbit of the preperiod-3 and period-1 Misiurewicz point $\mathrm{M}_{3,1}$, located at $c = -1.543689012692076\ldots$, is (CLR)L where we represent the preperiod in brackets followed by the period without brackets [8]. Then, the symbolic sequence of the orbit of the first Misiurewicz point –which corresponds to that of the least parameter absolute value– of preperiod-17 and period-8 $\mathrm{M}^{(1)}_{17,8}$, located at $c = -1.402492176358564\ldots$, is $(\mathrm{CLRL}^3\mathrm{RLRLRL}^3\mathrm{RL}^2)\mathrm{LRL}^3\mathrm{RLR}$. The symbolic sequence of the orbit of a Misiurewicz point for a given parameter value can also easily be obtained by direct iteration (note that the parameter precision in this case must be greater than the preceding one, because a Misiurewicz point is always unstable [8]).

2.3 About the harmonic notation

When the symbolic sequence is very long, it is useful to write it in a compact way, instead of an extended way. For that, we introduce a harmonic notation. In this way, the symbolic sequence of the period-16 superstable orbit of the period-doubling cascade, the fourth MSS-harmonic [13] of C, or the fourth iteration of the first F-harmonic of C [9], has the harmonic notation $H_{\mathrm{MSS}}^{(4)}(\mathrm{C})$ or $H_{\mathrm{F}}^{(1)\circ 4}(\mathrm{C})$. Indeed, $H_{\mathrm{MSS}}^{(1)}(\mathrm{C}) = H_{\mathrm{F}}^{(1)}(\mathrm{C}) = \mathrm{CL}$, $H_{\mathrm{MSS}}^{(2)}(\mathrm{C}) = H_{\mathrm{F}}^{(1)\circ 2}(\mathrm{C}) = \mathrm{CLRL}$, $H_{\mathrm{MSS}}^{(3)}(\mathrm{C}) = H_{\mathrm{F}}^{(1)\circ 3}(\mathrm{C}) = \mathrm{CLRL}^3\mathrm{RL}$, and $H_{\mathrm{MSS}}^{(4)}(\mathrm{C}) = H_{\mathrm{F}}^{(1)\circ 4}(\mathrm{C}) = \mathrm{CLRL}^3\mathrm{RLRLRL}^3\mathrm{RL}$.

Similarly, the harmonic notation of the orbits of the Misiurewicz points $\mathrm{M}_{2,1}^{(1)}$ (the end of the main antenna), $\mathrm{M}_{3,1}^{(1)}$ (it separates the chaotic bands $\mathbf{B}_0$ and $\mathbf{B}_1$ [7]), …, $\mathrm{M}_{17,8}^{(1)}$ (it separates $\mathbf{B}_3$ and $\mathbf{B}_4$), …, $\mathrm{M}_{2^{i+1}+1,2^{i-1}}^{(1)}$ (it separates $\mathbf{B}_i$ and $\mathbf{B}_{i+1}$), is the infinite F-harmonic of the corresponding superstable periodic orbit of the period-doubling cascade. Therefore, we have:

$$\mathrm{M}_{2,1} = (\mathrm{CL})\mathrm{R} = H_{\mathrm{F}}^{(\infty)}(\mathrm{C}),$$
$$\mathrm{M}_{3,1} = (\mathrm{CLR})\mathrm{L} = H_{\mathrm{F}}^{(\infty)}(H_{\mathrm{F}}^{(1)}(\mathrm{C})),$$
$$\mathrm{M}_{5,2}^{(1)} = (\mathrm{CLRL}^2)\mathrm{LR} = H_{\mathrm{H}}^{(\infty)}(H_{\mathrm{F}}^{(1)\circ 2}(\mathrm{C})),$$
$$\mathrm{M}_{9,4}^{(1)} = (\mathrm{CLRL}^3\mathrm{RLR})\mathrm{LRL}^2 = H_{\mathrm{F}}^{(\infty)}(H_{\mathrm{F}}^{(1)\circ 3}(\mathrm{C})),$$
$$\mathrm{M}_{17,8}^{(1)} = (\mathrm{CLRL}^3\mathrm{RLRLRL}^3\mathrm{RL}^2)\mathrm{LRL}^3\mathrm{RLR} = H_{\mathrm{F}}^{(\infty)}(H_{\mathrm{F}}^{(1)\circ 4}(\mathrm{C})).$$

Now, we shall illustrate some of the central features of the most important scaling constants.

3. IMPORTANT SCALING CONSTANTS

3.1 Feigenbaum scaling constant

It is well known that the Feigenbaum constant is $\delta_{\mathrm{F}} = 4.669201609103\ldots$ [1]. In Table 2 we have obtained this constant through the period-doubling cascade, by measuring the parameter values of the superstable orbits whose periods are 1, 2, 4, …, 1024, 2048 and

4096. In Fig. 2, a sketch of the Feigenbaum scaling constant in the Mandelbrot set through the period-doubling cascade (disks of periods 1024, 2048 and 4096) is shown using the Mandelbrot algorithm [14].

It is known as well that the chaotic bands also show bifurcation, called reverse bifurcation [15], as c increases from its lowest value $c=-2$ (the absolute value of c decreases). For $c=-1.54\ldots$ the single chaotic band splits into two, and for $c=-1.43\ldots$ the two chaotic bands split into four, and so forth, mimicking the period-doubling bifurcations observed for decreasing c (increasing the absolute value). In fact, each chaotic band is torn asunder by the surviving "ghost" of the corresponding period-doubling bifurcation [16]. The reverse bifurcation points of chaotic bands are the Misiurewicz points $\mathrm{M}^{(1)}_{2^i+1,2^{i-1}}$ $(i=0,1,2\ldots)$ [7]. In table 3, we show these points for $i\le 11$. When $c=\mathrm{M}^{(1)}_{513,256}$, the 256 chaotic bands split into 512; when $c=\mathrm{M}^{(1)}_{1025,512}$, the 512 chaotic bands split into 1024; finally, when $c=\mathrm{M}^{(1)}_{2049,1024}$, the 1024 chaotic bands split into 2048. It is not possible to show so many bifurcations in a figure. Therefore, in Fig. 3 (note its narrow vertical interval) only the bifurcation diagram of the upper chaotic band, using the Campbell [17] or the Collet and Eckmann [18] representation, is shown.

3.2. Scaling constant of the last appearance superstable periodic orbits

As is well known, different period-p superstable orbits exist. We call to the orbit with the least parameter absolute value the *first appearance* period-p orbit, and the orbit with the greatest parameter absolute value the *last appearance* period-p orbit, because they appear in the first and the last place when we increase the parameter absolute value c. The last appearance period-p superstable orbit in the period-1 chaotic band have the symbolic sequence CLR^{p-2} [16]. The scaling constant of these orbits, $\delta_{\mathrm{FPR}}=4.0$, was found by Frame *et al.* [19]. In Table 4 the superstable periodic orbits for $3\le p\le 16$ are shown. Note that these orbits accumulate at $c=-2$. In Fig. 4 we can not see the corresponding midgets, but we can see where they are located. This figure has been drawn using the escape line method [11].

3.3. Scaling constant of a sequence with two simultaneous limits

Geisel and Nierwetberg [20] studied the sequence of superstable orbits of periods $p = q \cdot 2^k$ where $k = 0,1,2,\ldots$ with k fixed, and $q = 3,4,5,\ldots$ If $k = 0$ then $p = 3,4,5,\ldots$, which are the periods of the last appearance superstable periodic orbits of the period-1 chaotic band (placed between the Misiurewicz points $\mathrm{M}_{2,1}^{(1)}$ and $\mathrm{M}_{3,1}^{(1)}$ [7]). When $k = i$ we have $p = 3 \cdot 2^i, 4 \cdot 2^i, 5 \cdot 2^i, \ldots$, which are the periods of the last appearance superstable periodic orbits of the period-2^i chaotic band (placed between the Misiurewicz points $\mathrm{M}_{2^i+1,2^{i-1}}^{(1)}$ and $\mathrm{M}_{2^{i+1}+1,2^i}^{(1)}$ [7]). The scaling constant of Geisel and Nierwetberg, $\delta_{\mathrm{GN}} = 2.94805...$ [20], corresponds to the sequence $p = q \cdot 2^k$ when simultaneously $k \to \infty$ and $q \to \infty$.

We have obtained this scaling constant in the period-2^7 chaotic band ($k = 7$), located between the Misiurewicz points $\mathrm{M}_{129,64}^{(1)}$ and $\mathrm{M}_{257,128}^{(1)}$, for the sequence $p = 3 \cdot 2^7, 4 \cdot 2^7, 5 \cdot 2^7, \ldots$ The results are shown in Table 5.

In Fig. 5 we have depicted the zone of the Mandelbrot set antenna where the period-1664, period-1792 and period-1920 midgets are placed. For that, the Milnor algorithm has been used [21]. The image corresponds to the surroundings of the Feigenbaum point; therefore, each point needed a large number of iterations (64000) and, as a result, the Fig. 5 is obtained very slowly. The midgets are so microscopic that they cannot be observed (their size are much smaller than the machine accuracy of the computer), but we can indirectly locate them by observing where the "tree trunks" of what we call "Milnor-Feigenbaum forest" are placed.

3.4. Scaling constants of multifurcations

Multifurcations are an extent of bifurcations. Feigenbaum studied the bifurcations of the period-doubling cascade [1], where the periods (1, 2, 4, 8, 16,…) increase according to powers of 2. A little later, Derrida *et al.* studied the trifurcations [22], where the periods (1, 3, 9, 27, 81, 243, …) increase according to powers of 3. The main antenna of the Mandelbrot set has a period-3 midget. In its turn, this midget has its antenna, where there is another much smaller midget of period 9. In turn, this midget also has its antenna, where there is another much smaller midget of period 27. And so on. Derrida *et*

al. [22] found the scaling constant value of the trifurcations $\delta_{3f} = 55.247\ldots$ We also have obtained this constant as can be seen in Table 6, where the symbolic sequences are given in a compact form by using the notation of Derrida *et al.* [22] that they denote *. In Fig. 6, a sketch of the scaling constant of trifurcations, using the Mandelbrot algorithm [14], is shown.

As is well known, there are three period-5 midgets in the Mandelbrot set antenna. Hence, there are three different scaling constants in the pentafurcations ($\delta_{5f}^{1)} = 255.5$, $\delta_{5f}^{2)} = 1287$ y $\delta_{5f}^{3)} = 16930$) as has been shown by Sousa [23]. Let us note that the scaling constant values of the multifurcations are very large (we could speak of scaling megaconstants). The theory of period doubling for real iterative mappings has been generalized to period *n*-tupling for complex iterative mappings by Cvitanovic *et al.* [24], and Milnor [21] has studied the limit point (a generalized Feigenbaum point) of the sequence of multifurcations in the complex plane.

4. A SCALING CONSTANT EQUAL TO UNITY

Close to the cusp of the period-3 midget in the Mandelbrot set antenna [10], there are two sequences of microscopic midgets that have a scaling constant whose value presumably is the unity: one of them is $C\overline{CLRL}L$, $C\overline{CLRL}^{2}L$, $C\overline{CLRL}^{3}L$, … (of periods 5, 8, 11, …), and the other is $C\overline{CLRL}^{2}$, $C\overline{CLRL}^{3}$, $C\overline{CLRL}^{4}$,… (of periods 7, 10, 13, …). It is known that the part of the Mandelbrot set corresponding to the neighborhood of one of these midgets shows a complex branching structure (see Fig. 1 of ref. [25], and Figs. 9 and 10 of ref. [11]). It is easy to see that the period of the midget placed in the middle of the Fig. 1 of ref. [25] is 203, and that its symbolic sequence is $C\overline{CLRL}^{67}L$. In Fig. 7, the neighborhood of this midget has been drawn by means of the escape line method [11] in order to compare it with the Fig. 1 of ref. [25] that was drawn by means of the Milnor algorithm. The midget is very small and therefore is not visible (the diameter of its main cardioid is about 2.4×10^{-10}), even though its position can easily be detected.

In Table 7, six values for the scaling constants of triads $C\overline{CLRL}^{\alpha}L$, $C\overline{CLRL}^{\alpha+1}L$ and $C\overline{CLRL}^{\alpha+2}L$ ($\alpha = 2, 32, 128, 512, 2048$ and 4096) of the $C\overline{CLRL}^{2}L$, $C\overline{CLRL}^{3}L$, $C\overline{CLRL}^{4}L$, $C\overline{CLRL}^{5}L$ … scaling has been obtained. The convergence is very slow; therefore, the

constants could not be determined with the precision we wanted. For the orbits of the triad $C\overline{LRL}^{4096}L$, $C\overline{LRL}^{4097}L$ and $C\overline{LRL}^{4098}L$ we obtained the value $\delta_u = 1.000\ldots$, and hence we conjecture that in the limit, when the periods of the orbits tend to infinity, this scaling constant is equal to unity. In Fig. 8, a sketch of this scaling constant is shown.

While at first they may seem impossible, bounded sequences with scaling factor 1 are easy to construct. For example, let $c_n = -1.75 + (1/n^2)$. Note as $n \to \infty$, $c_n \to -1.75$. Also note $|c_{n-1} - c_n| / |c_n - c_{n+1}| \to 1$ as $n \to \infty$. While not a model for the scaling reported in this paper, this simple example shows a bounded sequence can have a scaling of 1.

The approach to scaling constants pioneered by Feigenbaum is based on computing the unstable eigenvalue of a renormalization operator. In some cases, however, a much more elementary approach can work. In particular, if the scaling constant appears to be an integer, we like to believe there should be a way to discover this integer encoded in some fundamental way in the iteration process. For example, the scaling reported by Frame, Philip and Robucci [19] was later explained in this way by Hurwitz, Frame and Peak [26]. For future work, we shall try to find an analogous explanation for the scaling constant reported in this work.

5. CONCLUSIONS

After an introduction about scaling constants, some previous considerations that make it possible to do this work have been made. Thus, the computer precision and the symbolic sequences have been treated. The harmonic notation has been introduced. We deal with the well known Feigenbaum scaling constant [1] and other important scaling constants: the scaling constant of the last appearance superstable periodic orbits, the scaling constant with two simultaneous limits, and the scaling constant of the trifurcations. We illustrate some of the central features of these scaling constants.

Finally, we introduce a new scaling constant with a notable property: its value is, presumably, the unity. We can point out two features about this result. Firstly, this scaling constant is an integer, as the Frame *et al.* scaling constant; and, secondly, it reaches the lowest possible value.

ACKNOWLEDGMENTS

This work was supported by CICYT and DGICYT, Spain, under grants No. TIC95-0080 and PB94-0045 respectively.

REFERENCES

1. M. J. Feigenbaum, Quantitative universality for a class of nonlinear transformations, *J. Stat. Phys.* **19**, 25-52 (1978).
2. K. Briggs, How to calculate the Feigenbaum constants on your PC, *Aust. Math. Soc. Gazette* **16**, 89 (1989).
3. K. Briggs, A precise calculation of the Feigenbaum constants, *Math. Comput.* **57**, 435-439 (1991).
4. H.-O. Peitgen, H. Jürgens and D. Saupe, *Chaos and Fractals*, Springer-Verlag, New York (1992).
5. J. Milnor and W. Thuston, On iterated maps of the interval, *Lect. Notes Math.* **1342**, 465-563 (1988).
6. R. L. Devaney, *Chaotic Dynamical Systems* (Addison-Wesley, second edition, 1989).
7. G. Pastor, M. Romera and F. Montoya, An approach to the ordering of one-dimensional quadratic maps, *Chaos Solitons and Fractals* **7**, 565-584 (1996).
8. M. Romera, G. Pastor and F. Montoya, Misiurewicz points in one-dimensional quadratic maps, *Physica A* **232**, 517-535 (1996).
9. G. Pastor, M. Romera and F. Montoya, On the calculation of Misiurewicz pattern in one-dimensional quadratic maps, *Physica A* **232,** 536-553 (1996).
10. M. Romera, G. Pastor and F. Montoya, On the cusp and the tip of a midget in the Mandelbrot set antenna, *Phys. Lett. A*, **221**, 158-162 (1996).
11. M. Romera, G. Pastor and F. Montoya, Graphic tools to analyse one-dimensional quadratic maps, *Computers & Graphics* **20**, 333-339 (1996).
12. W. H. Press, B. P. Flannery, S. A. Teukolsky and W. T. Vetterling, *Numerical Recipes in C*, Cambridge University Press, Cambridge (1988).
13. N. Metropolis, M. L. Stein and P. R. Stein, On finite limit sets for transformations on the unit interval, *J. Comb. Theory* **15**, 25-44 (1973).

14. B. B. Mandelbrot, On the quadratic mapping $z \mapsto z^2 - \mu$ for complex μ and z: the fractal structure of its M set, and scaling, *Physica D* **7**, 224–239 (1983).
15. E. N. Lorenz, Noisy periodicity and reverse bifurcation, *Ann. NY. Acad. Sci.* **357**, 282-291 (1980).
16. M. Schroeder, *Fractals, Chaos, Power Laws*, W. H. Freeman, New York (1991).
17. D. Campbell, An Introduction to Nonlinear Dynamics. In *Lectures in the Sciences of Complexity*, D. L. Stein (Ed.), Addison-Wesley, Reading, MA (1979).
18. P. Collet and J.-P Eckmann, *Iterated Maps on the Interval as Dynamical Systems*, Birkhäuser, Boston (1980).
19. M. Frame, A. G. D. Philip and A. Robucci, A new scaling along the spike of the Mandelbrot set, *Computers & Graphics* **16,** 223–234 (1992).
20. T. Geisel and J. Nierwetberg, Universal fine structure of chaotic region in period-doubling systems, *Phys. Rev. Lett.* **47**, 975-978 (1981).
21. J. Milnor, Self-similarity and hairiness in the Mandelbrot set, *Lecture Notes in Pure and Applied Mathematics* **114**, 211–257 (1989).
22. B. Derrida, A. Gervois and Y. Pomeau, Universal metric properties of bifurcations of endomorphisms, *J. Phys. A-Math. Gen.* **12**, 269-296 (1979).
23. M. C. de Sousa Vieira, Scaling factors associated with *m*-furcations of the $1 - \mu|x|^z$ map, *J. Stat. Phys.* **53**, 1315-1325 (1988).
24. P. Cvitanovic and J. Myrheim, Universality for period *n*-tuplings in complex mappings, *Phys. Lett. A* **94**, 329-333 (1983).
25. M. Frame and A. Robucci, Complex branchings. In *The pattern book*, C. Pickover (Ed.), World Scientific, Singapore, 231-232 (1995).
26. H. Hurwitz, M. Frame and D. Peak, Scaling symmetries in nonlinear dynamics. A view from parameter space, *Physica D* **81**, 23-31 (1995).

Table 1. Test of the computer precision used in this work.

Operation	$1.11111111 \times 1.11111111$	$9.99999999 \times 9.99999999$
Computed value	$\overset{1\ 2\ 3\ 4\ 5\ 6\ 7\ 8\ 9\ 10\ 11\ 12\ 13\ 14\ 15\ 16\ 17}{1.2345678987654320 0}$	$\overset{1\ 2\ 3\ 4\ 5\ 6\ 7\ 8\ 9\ 10\ 11\ 12\ 13\ 14\ 15\ 16\ 17}{9.9999999799999983 4} \times 10^{1}$
Exact value	$\overset{1\ 2\ 3\ 4\ 5\ 6\ 7\ 8\ 9\ 10\ 11\ 12\ 13\ 14\ 15\ 16\ 17}{1.2345678987654321 0}$	$\overset{1\ 2\ 3\ 4\ 5\ 6\ 7\ 8\ 9\ 10\ 11\ 12\ 13\ 14\ 15\ 16\ 17}{9.9999999800000000 01} \times 10^{1}$

Table 2. Map $x_{n+1} = x_n^2 + c$. Feigenbaum scaling constant through the period-doubling cascade.

Period p	Harmonic notation	Parameter c	Parameter increment $\lvert\Delta c\rvert$	δ_{F}
1	C	0		
2	$H_{\mathrm{F}}^{(1)}(\mathrm{C})$	–1.0	1.0	
4	$H_{\mathrm{F}}^{(1)\circ 2}(\mathrm{C})$	–1.310702641336832…	$3.10702641336832\ldots 10^{-2}$	3.218511…
8	$H_{\mathrm{F}}^{(1)\circ 3}(\mathrm{C})$	–1.381547484432061…	$7.0844843095229\ldots 10^{-2}$	4.385677…
16	$H_{\mathrm{F}}^{(1)\circ 4}(\mathrm{C})$	–1.396945359704560…	$1.5397875272499\ldots 10^{-2}$	4.600949…
32	$H_{\mathrm{F}}^{(1)\circ 5}(\mathrm{C})$	–1.400253081214782…	$3.307721510222\ldots 10^{-3}$	4.655130…
64	$H_{\mathrm{F}}^{(1)\circ 6}(\mathrm{C})$	–1.400961962944841…	$7.08881730059\ldots 10^{-4}$	4.666111…
128	$H_{\mathrm{F}}^{(1)\circ 7}(\mathrm{C})$	–1.401113804939776…	$1.51841994935\ldots 10^{-4}$	4.668548…
256	$H_{\mathrm{F}}^{(1)\circ 8}(\mathrm{C})$	–1.401146325826946…	$3.2520887170\ldots 10^{-5}$	4.669060…
512	$H_{\mathrm{F}}^{(1)\circ 9}(\mathrm{C})$	–1.401153290849923…	$6.965022977\ldots 10^{-6}$	4.669171…
1024	$H_{\mathrm{F}}^{(1)\circ 10}(\mathrm{C})$	–1.401154782546617…	$1.491696694\ldots 10^{-6}$	4.669195…
2048	$H_{\mathrm{F}}^{(1)\circ 11}(\mathrm{C})$	–1.401155102022463…	$3.19475846\ldots 10^{-7}$	4.669200…
4096	$H_{\mathrm{F}}^{(1)\circ 12}(\mathrm{C})$	–1.401155170444411…	$6.8421948\ldots 10^{-8}$	4.669201…

Table 3. Map $x_{n+1} = x_n^2 + c$. Feigenbaum scaling constant through the inverse bifurcation of chaotic bands.

Misiurewicz point	Harmonic notation	Parameter c	Parameter increment $\lvert\Delta c\rvert$	δ_{F}
$\mathrm{M}_{2,1}^{(1)}$	$H_{\mathrm{F}}^{(\infty)}(\mathrm{C})$	–2.00000000000000…		
$\mathrm{M}_{3,1}^{(1)}$	$H_{\mathrm{F}}^{(\infty)}(H_{\mathrm{F}}^{(1)}(\mathrm{C}))$	–1.543689012692076…	4.56310987307924… 10^{-1}	
$\mathrm{M}_{5,2}^{(1)}$	$H_{\mathrm{F}}^{(\infty)}(H_{\mathrm{F}}^{(1)\circ 2}(\mathrm{C}))$	–1.430357632451307…	1.13331380240769… 10^{-1}	4.026342…
$\mathrm{M}_{9,4}^{(1)}$	$H_{\mathrm{F}}^{(\infty)}(H_{\mathrm{F}}^{(1)\circ 3}(\mathrm{C}))$	–1.407405118164702…	2.2952514286605… 10^{-2}	4.937645…
$\mathrm{M}_{17,8}^{(1)}$	$H_{\mathrm{F}}^{(\infty)}(H_{\mathrm{F}}^{(1)\circ 4}(\mathrm{C}))$	–1.402492176358564…	5.012941806138… 10^{-3}	4.578651…
$\mathrm{M}_{33,16}^{(1)}$	$H_{\mathrm{F}}^{(\infty)}(H_{\mathrm{F}}^{(1)\circ 5}(\mathrm{C}))$	–1.401441494253588…	1.050682104976… 10^{-3}	4.771130…
$\mathrm{M}_{65,32}^{(1)}$	$H_{\mathrm{F}}^{(\infty)}(H_{\mathrm{F}}^{(1)\circ 6}(\mathrm{C}))$	–1.401216504309415…	2.24989944173… 10^{-4}	4.669906…
$\mathrm{M}_{129,64}^{(1)}$	$H_{\mathrm{F}}^{(\infty)}(H_{\mathrm{F}}^{(1)\circ 7}(\mathrm{C}))$	–1.401168320839301…	4.8183470114… 10^{-5}	4.669442…
$\mathrm{M}_{257,128}^{(1)}$	$H_{\mathrm{F}}^{(\infty)}(H_{\mathrm{F}}^{(1)\circ 8}(\mathrm{C}))$	–1.401158001505211…	1.0319334090… 10^{-5}	4.669242…
$\mathrm{M}_{513,256}^{(1)}$	$H_{\mathrm{F}}^{(\infty)}(H_{\mathrm{F}}^{(1)\circ 9}(\mathrm{C}))$	–1.401155791424613…	2.210080598… 10^{-6}	4.669211…
$\mathrm{M}_{1025,512}^{(1)}$	$H_{\mathrm{F}}^{(\infty)}(H_{\mathrm{F}}^{(1)\circ 10}(\mathrm{C}))$	–1.401155318093230…	4.73331383… 10^{-7}	4.669203…
$\mathrm{M}_{2049,1024}^{(1)}$	$H_{\mathrm{F}}^{(\infty)}(H_{\mathrm{F}}^{(1)\circ 11}(\mathrm{C}))$	–1.401155216720152…	1.01373078… 10^{-7}	4.669202…

Table 4. Map $x_{n+1} = x_n^2 + c$. Frame, Philip and Robucci scaling constant through the last appearance periodic orbits of the period-1 chaotic band.

Period p	Symbolic sequence	Parameter c	Parameter increment $\lvert\Delta c\rvert$	δ_{FPR}
3	CLR	-1.754877666246692…		
4	CLR^2	-1.940799806529484…	1.85922140282792… 10^{-1}	
5	CLR^3	-1.985424253054205…	4.4624446524721… 10^{-2}	4.166374…
6	CLR^4	-1.996376137711193…	1.0951884656988… 10^{-2}	4.074590…
7	CLR^5	-1.999095682327018…	2.719544615925… 10^{-3}	4.027102…
8	CLR^6	-1.999774048693727…	6.78366366709… 10^{-4}	4.008961…
9	CLR^7	-1.999943521765674…	1.69473071947… 10^{-4}	4.002797…
10	CLR^8	-1.999985881140392…	4.2359374718… 10^{-5}	4.000839…
11	CLR^9	-1.999996470335008…	1.0589194616… 10^{-5}	4.000245…
12	CLR^{10}	-1.999999117587260…	2.647252252… 10^{-6}	4.000070…
13	CLR^{11}	-1.999999779397058…	6.61809798… 10^{-7}	4.000019…
14	CLR^{12}	-1.999999944849281…	1.65452223… 10^{-7}	4.000005…
15	CLR^{13}	-1.999999986212321…	4.1363040… 10^{-8}	4.000001…
16	CLR^{14}	-1.999999996553080…	1.0340759… 10^{-8}	4.000000…

Table 5. Map $x_{n+1} = x_n^2 + c$. Geisel and Nierwetberg scaling constant through the last appearance superstable periodic orbits of the period-2^7 chaotic band.

Period p	Harmonic notation	Parameter c	Parameter increment $\lvert\Delta c\rvert$	δ_{GN}
384	$H_{\mathrm{F}}^{(2)}[H_{\mathrm{F}}^{(1)\circ 7}(\mathrm{C})]$	–1.401162303032819…		
512	$H_{\mathrm{F}}^{(3)}[H_{\mathrm{F}}^{(1)\circ 7}(\mathrm{C})]$	–1.401166466451837…	4.163319018… 10^{-6}	
640	$H_{\mathrm{F}}^{(4)}[H_{\mathrm{F}}^{(1)\circ 7}(\mathrm{C})]$	–1.401167717185749…	1.250733912… 10^{-6}	3.3288…
768	$H_{\mathrm{F}}^{(5)}[H_{\mathrm{F}}^{(1)\circ 7}(\mathrm{C})]$	–1.401168119587305…	4.02401566… 10^{-7}	3.1081…
896	$H_{\mathrm{F}}^{(6)}[H_{\mathrm{F}}^{(1)\circ 7}(\mathrm{C})]$	–1.401168253056095…	1.3346879… 10^{-7}	3.0149…
1024	$H_{\mathrm{F}}^{(7)}[H_{\mathrm{F}}^{(1)\circ 7}(\mathrm{C})]$	–1.401168297912099…	4.4856004… 10^{-8}	2.9755…
1152	$H_{\mathrm{F}}^{(8)}[H_{\mathrm{F}}^{(1)\circ 7}(\mathrm{C})]$	–1.401168313070917…	1.5158818… 10^{-8}	2.9592…
1280	$H_{\mathrm{F}}^{(9)}[H_{\mathrm{F}}^{(1)\circ 7}(\mathrm{C})]$	–1.401168318205346…	5.134429… 10^{-9}	2.9522…
1408	$H_{\mathrm{F}}^{(10)}[H_{\mathrm{F}}^{(1)\circ 7}(\mathrm{C})]$	–1.401168319945991…	1.740645… 10^{-9}	2.9497…
1536	$H_{\mathrm{F}}^{(11)}[H_{\mathrm{F}}^{(1)\circ 7}(\mathrm{C})]$	–1.401168320536302…	5.90311… 10^{-10}	2.9486…
1664	$H_{\mathrm{F}}^{(12)}[H_{\mathrm{F}}^{(1)\circ 7}(\mathrm{C})]$	–1.401168320736524…	2.00222… 10^{-10}	2.9483…
1792	$H_{\mathrm{F}}^{(13)}[H_{\mathrm{F}}^{(1)\circ 7}(\mathrm{C})]$	–1.401168320804438…	6.7914… 10^{-11}	2.9481…
1920	$H_{\mathrm{F}}^{(14)}[H_{\mathrm{F}}^{(1)\circ 7}(\mathrm{C})]$	–1.401168320827475…	2.3037… 10^{-11}	2.9480…

Table 6. Map $x_{n+1} = x_n^2 + c$. Derrida, Gervois and Pomeau scaling constant of trifurcations.

Period p	Symbolic sequence	Parameter c	Parameter increment $\lvert\Delta c\rvert$	δ_{3f}
3	CLR	-1.75487766624669…		
9	$\overline{\text{CLR}}^{*2}$	-1.78586564641067…	3.098798016398… 10^{-2}	
27	$\overline{\text{CLR}}^{*3}$	-1.78642985805576…	5.6421164509… 10^{-4}	54.92…
81	$\overline{\text{CLR}}^{*4}$	-1.78644006735907…	1.020930331… 10^{-5}	55.26…
243	$\overline{\text{CLR}}^{*5}$	-1.78644025215704…	1.8479797… 10^{-7}	55.24…

Table 7. Map $x_{n+1} = x_n^2 + c$. Unity scaling constant close to the period-three tangent bifurcation.

Period p	Symbolic sequence	Parameter c	Parameter increment $\lvert\Delta c\rvert$	δ_u
8	$C\overline{LRL}^{2}L$	–1.711079470013152…		
11	$C\overline{LRL}^{3}L$	–1.732006272869656…	2.0926802856504… 10^{-2}	
14	$C\overline{LRL}^{4}L$	–1.739717601451463…	0.7711328581807… 10^{-2}	2.713…
98	$C\overline{LRL}^{32}L$	–1.749814314576552…		
101	$C\overline{LRL}^{33}L$	–1.749825129737434…	1.0815160882… 10^{-5}	
104	$C\overline{LRL}^{34}L$	–1.749835025064937…	0.9895327503… 10^{-5}	1.092…
386	$C\overline{LRL}^{128}L$	–1.749987898954803…		
389	$C\overline{LRL}^{129}L$	–1.749988084425097…	1.85471294… 10^{-7}	
392	$C\overline{LRL}^{130}L$	–1.749988265663272…	1.81238175… 10^{-7}	1.023…
1538	$C\overline{LRL}^{512}L$	–1.749999234738764…		
1541	$C\overline{LRL}^{513}L$	–1.749999237713374…	2.974610… 10^{-9}	
1544	$C\overline{LRL}^{514}L$	–1.749999240670673…	2.957289… 10^{-9}	1.005…
6146	$C\overline{LRL}^{2048}L$	–1.749999952026344…		
6149	$C\overline{LRL}^{2049}L$	–1.749999952073135…	4.6791… 10^{-11}	
6152	$C\overline{LRL}^{2050}L$	–1.749999952119858…	4.6723… 10^{-11}	1.001…
12290	$C\overline{LRL}^{4096}L$	–1.749999988000501…		
12293	$C\overline{LRL}^{4097}L$	–1.749999988006357…	5.856… 10^{-12}	
12296	$C\overline{LRL}^{4098}L$	–1.749999988012208…	5.851… 10^{-12}	1.000…

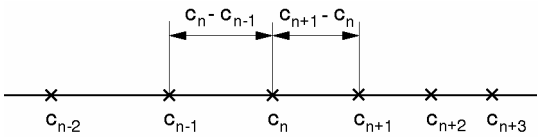

Fig. 1. A sketch of scaling constant. $\delta_n = |c_n - c_{n-1}| / |c_{n+1} - c_n|$.

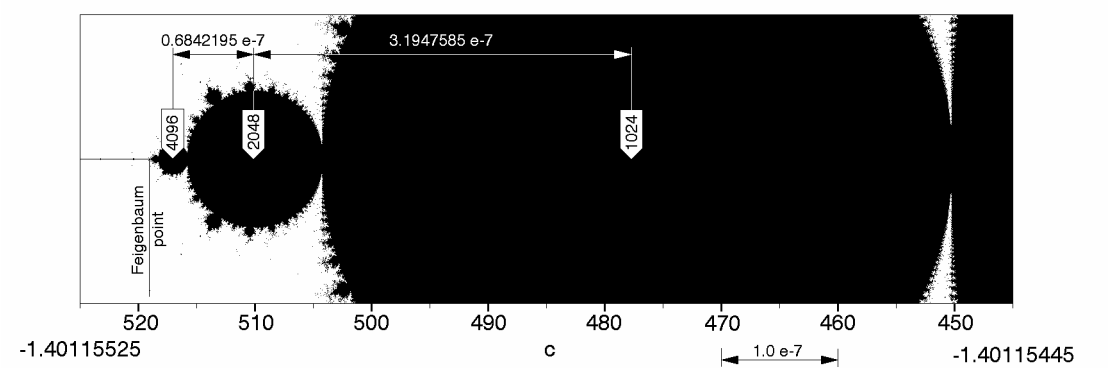

Fig. 2. A sketch of the Feigenbaum scaling constant in the Mandelbrot set through the period-doubling cascade. $\delta_{\mathrm{F}} = 3.1947585\ldots\times10^{-7}/0.6842195\ldots\times10^{-7} = 4.669201\ldots$

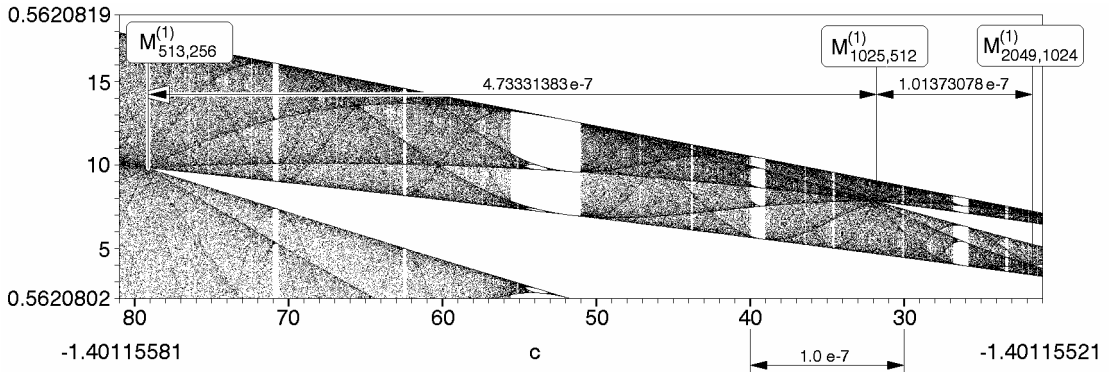

Fig. 3. A sketch of the Feigenbaum scaling constant in the real Mandelbrot map $x_{n+1} = x_n^2 + c$ through the inverse bifurcation of chaotic bands. $\delta_F = 4.73331383\ldots\times10^{-7}/1.01373078\ldots\times10^{-7} = 4.669202\ldots$

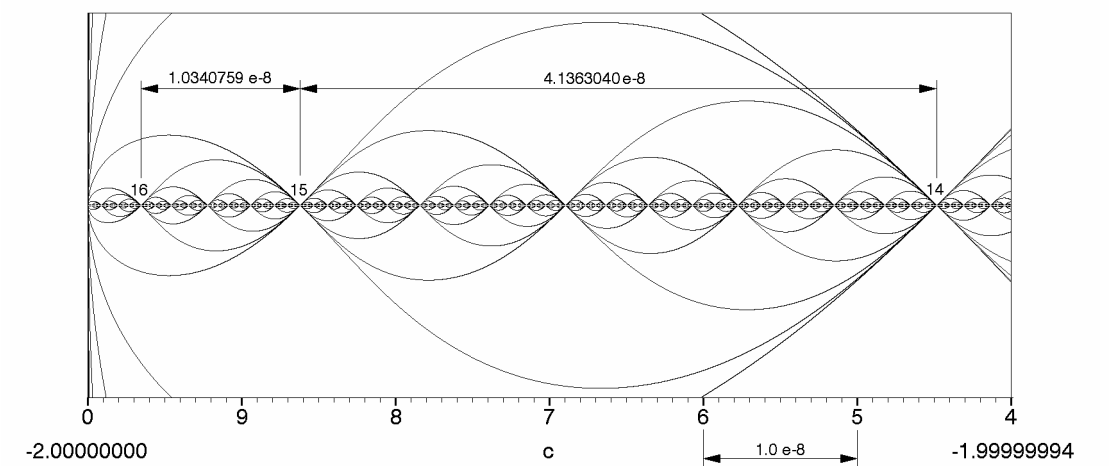

Fig. 4. A sketch of the Frame, Philip and Robucci scaling constant in the Mandelbrot set through the last appearance midgets of the period-1 chaotic band. $\delta_{\mathrm{FPR}} = 4.1363040\ldots\times10^{-8}/1.0340759\ldots\times10^{-8} = 4.000000\ldots$

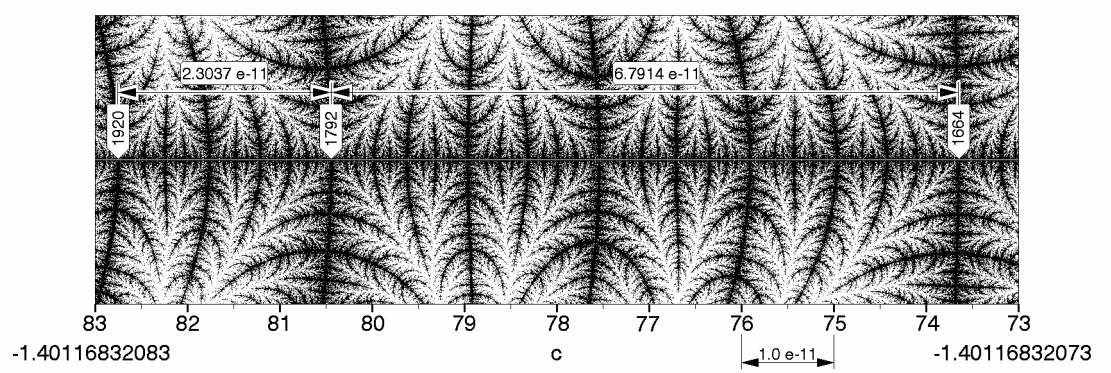

Fig. 5. A sketch of the Geisel and Nierwetberg scaling constant in the Mandelbrot set through the last appearance midgets of the period- 2^7 chaotic band. $\delta_{GN} = 6.7914\ldots\times10^{-11}/2.3037\ldots\times10^{-11} = 2.9480\ldots$

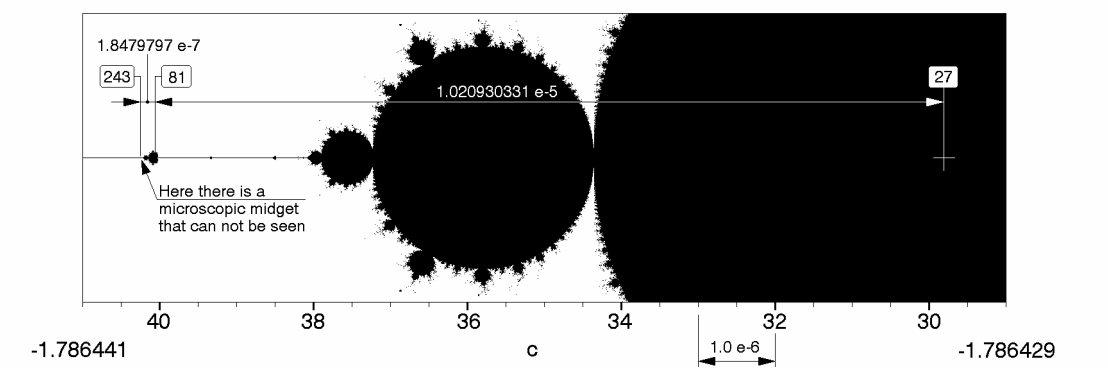

Fig. 6. A sketch of the scaling constant of trifurcations in the Mandelbrot set. $\delta_{3f} = 1.020930331\ldots\times10^{-5}/1.8479797\ldots\times10^{-7} = 55.24\ldots$

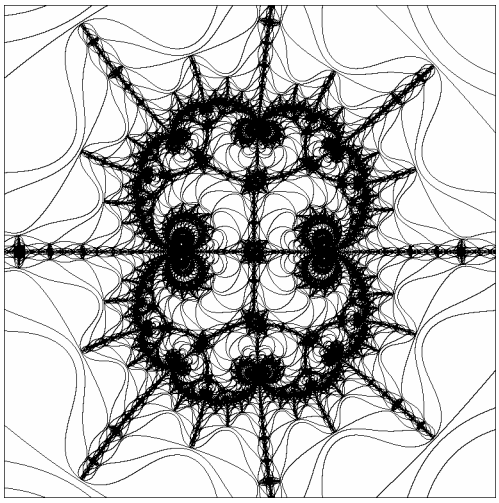

Fig. 7. The neighborhood of the period-203 $\overline{\text{CLRL}^{67}\text{L}}$ midget in the Mandelbrot set antenna, located at $c = -1.749956428438686\ldots$. The picture is drawn by the escape line method, is centered at $c = -1.74995643$, and its width is 2.0×10^{-7}.

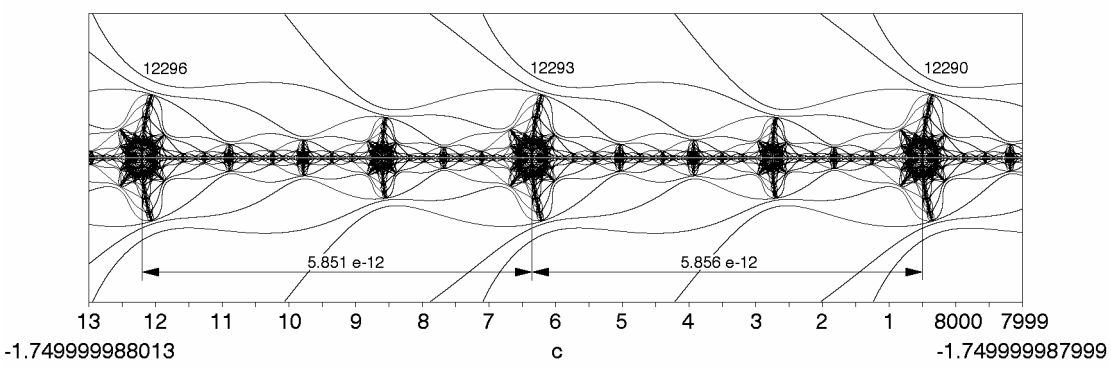

Fig. 8. A sketch of the scaling constant, presumably equal to unity, close to the cusp of the period-3 midget of the Mandelbrot set. $\delta_u = 5.856\ldots\times10^{-12}/5.851\ldots\times10^{-12} = 1.000\ldots$